25th ABCM International Congress of Mechanical Engineering
October 20-25, 2019, Uberlândia, MG, Brazil

GUST ALLEVIATION BASED ON MAGNETORHEOLOGICAL DAMPERS AND LINEAR MATRIX INEQUALITIES

Pedro Henrique Foster Stangarlin[1]
Frederico Albuquerque Ribeiro[2]
Douglas Domingues Bueno[3]
São Paulo State University (Unesp), School of Engineering of Ilha Solteira. Av. Brasil, 56, Ilha Solteira, SP, 15385-000, BR
pedro.foster@unesp.br[1]
frederico.a.ribeiro@unesp.br[2]
douglas.bueno@unesp.br[3]
Abstract. *Gust loads can compromise the structural integrity of an aircraft in flight and because of this gust alleviation is a relevant area for engineers. Typically, aircraft flights through a different flight planning when atmosphere turbulence is detected. However, in general is not possible to avoid this type of condition, and on board control technologies are a good strategy to keep a safety flight. In this context, this work investigate the use of and approach based on linear matrix inequalities (LMI) and magnetorheological damper (MRD) to design a controller. It is considered to a 3 DOF (degrees of freedom) airfoil and 1-cosine gust to evaluated the system responses. The results show that the strategy is efficient to dissipate this kind of gust load.*

Keywords: *aeroelasticity, magnetorheological damper, gust,* $1 - cosine$*, LMI, control*

1. INTRODUCTION

Aeroelastic is the subject that describes the interaction of aerodynamic, inertia and elastic force for a flexible structure and has been applied to and important class of problems in airplane design (Bisplinghoff *et al.*, 1996; Wright and Cooper, 2007). One of aeroelastic phenomena is the gust or turbulence, these phenomena attract the attention of the engineering community to design and apply gust alleviation systems to provide comfort and guarantee structural integrity of aircraft (Regan and Jutte, 2012; Suleman and Costa, 2004; Guo *et al.*, 2015).

During the years, many researches have been carried out to develop active control systems for controlling aeroelastic response (Karpel, 1981). Gust, like atmospheric turbulence, may give rise to aircraft passenger discomfort and will introduce internal loads that need to be considered in the flight path. Thus it is important for and aircraft safe design to calculate de response generated under the conditions defined by the regulatory agencies (Wright and Cooper, 2007).

Magnetorheological dampers (MRD) are semi-active devices to provide energy dissipation through changing the resistance of the fluid, turning the fluid into a semi-solid as a function of the electric current, or electrical voltage, input (Jansen and Dyke, 2000). MRDs to provide vibration control are used in many different engineering areas, such as vehicles suspensions, bridges and buildings for seismic protection (Spencer Jr. *et al.*, 1996; Dyke *et al.*, 1998).

In particular, this work proposes to use the Clipped-Optimal control method for magnetorheological damper (MRD) (Dyke *et al.*, 1996) combined with linear matrix inequalities (LMI) to promote 1-cosine gust alleviation in a three degrees of freedom (3 DOF) airfoil.

2. METHODOLOGY

The aeroelastic equation of motion for the system illustrated by the Fig. 1 is given by Eq. (1), where, $\mathbf{M}$ is the mass matrix, $\mathbf{B}$ is the damping matrix, $\mathbf{K}$ is the stiffness matrix, $\mathbf{u}(t) = \{h(t) \quad \theta(t) \quad \beta(t)\}^T$ is the displacement vector, $q = \frac{1}{2}\rho V^2$ is the dynamic pressure, $\mathbf{Q}$ the aerodynamic influence coefficients matrix (AIC) defined by Theodorsen (1935) for each reduced frequency domain $k = \dfrac{\omega b}{V}$, V is the airspeed, ρ is the air density and b is the semi chord. $\mathbf{F}_{mrd}(t)$ is MRD force vector and $\mathbf{F}_g(t)$ is the gust load vector. Table 1 presents physical and geometrical properties of the 3DOF typical section.

$$\mathbf{M}\ddot{\mathbf{u}}(t) + \mathbf{B}\dot{\mathbf{u}}(t) + \mathbf{K}\mathbf{u}(t) + \mathbf{F}_{mrd}(t) = q\mathbf{Q}(k)\mathbf{u}(t) + \mathbf{F}_g(t) \tag{1}$$

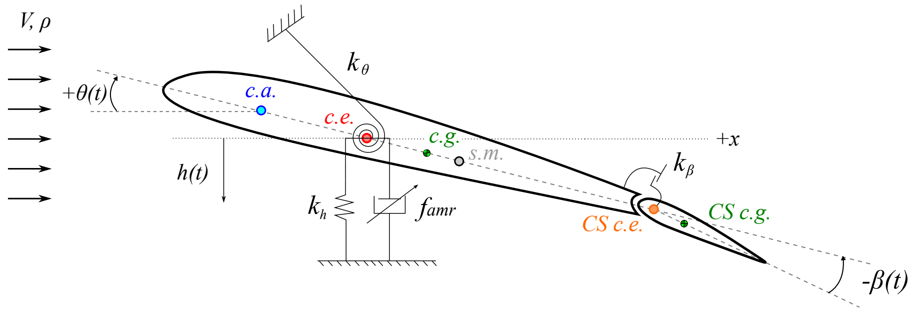

Figure 1. 3DOF system illustration.

Table 1. Three DOF typical section airfiol physical and geometric properties.

Parameter	**Value**
airfoil semi-chord	$b = 0.7m$
airfoil mass	$m = 20kg$
plunge frequency	$f_h = 5.5Hz$
pitch frequency	$f_\theta = 11Hz$
surface control frequency	$f_\beta = 20Hz$
c.e measured from s.m	$a = -0.4$
location of CS c.e measured from s.m	$c = 0.6$
c.g from c.g	$x_\theta = 0.2$
CS c.g coordinate from c.e	$x_\beta = 0.0125$
radius of gyration of the airfoil referred to a a	$r = (0.25)^{1/2}$
radius of gyration of the CS referred to the hinge a	$r = (0.00625)^{1/2}$
air density	$\rho = 1.225kg/m^3$

The Theodorsen's matrix $\mathbf{Q}(k)$ can not be transformed to time domain directly to obtain the system time domain representation. Therefore, an approximation method can be used to obtain the time domain representation of the aerodynamic forces. For this work the approximation method applied is the Least Square, also known as Roger-Abel method (Roger, 1977; Abel, 1979). These authors propose the Laplace invertible rational function shown in the Eq. (2):

$$\mathbf{Q}_{app}(s) = \mathbf{Q}_0 + \mathbf{Q}_1 s\left(\frac{b}{V}\right) + \mathbf{Q}_2 s^2\left(\frac{b}{V}\right)^2 + \sum_{j=1}^{n_{lag}} \mathbf{Q}_{(j+2)}\left(\frac{s}{s+\frac{V}{b}\gamma_j}\right) \tag{2}$$

where the coefficients $\mathbf{Q}_0$, $\mathbf{Q}_1$, $\mathbf{Q}_2$ and $\mathbf{Q}_{j+2}$ are calculated using a Least square method. The γ_j are the lag parameters selected using an empirical equation (Eq. 3, Chen (2000)) to calculate the values of γ_j based on the number of lag parameters and the largest reduced frequency considered to solve the problem.

$$\gamma_j = 1{,}7k_{max}\left(\frac{j}{n_{lag}+1}\right)^2 \tag{3}$$

For this system is used 7 lag parameters to get accurate approximation. The system representation in space-state is given by:

$$\dot{\mathbf{x}}(t) = \mathbf{A}\mathbf{x}(t) + \mathbf{B}_m\mathbf{F}_{mrd}(t) + \mathbf{B}_g\mathbf{F}_g(t) \tag{4}$$

where, $\mathbf{A}$ is the aeroelastic dynamic matrix, $\mathbf{B}_m$ and $\mathbf{B}_g$ are, respectively the input matrix for MR damper and gust (see appendix A).

The 1-cosine gust force, as shown in Fig. 2, is defined by (Wright and Cooper, 2007), considering a vertical displacement component $h(t)$:

$$W_g(t) = \pi\rho V(2b)V_g(t) \tag{5}$$

where is the vertical speed $V_g(t)$ defined the following equation:

$$V_g(t) = \begin{cases} \frac{A_g V}{2}\left[1-\cos\left(\frac{2\pi V t}{2H}\right)\right], & 0 \le t \le \frac{2H}{V} \\ 0 & t > \frac{2H}{V} \end{cases} \tag{6}$$

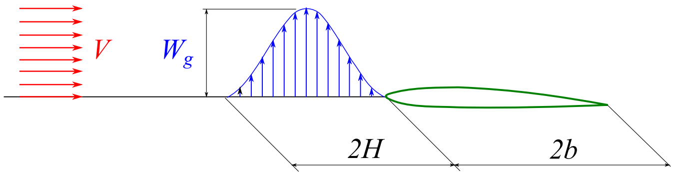

Figure 2. Gust effect illustration, where V is flow velocity.

where H is the gust gradient, i.e., the distance from the beginning to its maximum value and A_g is a value between 0 and 1 that define the maximum gust 1-cosine speed magnitude in terms of V.

The MRD (magneto rheological damper) mathematical model of force described by Eq. (7) and detailed presentation by Spencer Jr. *et al.* (1996), as shown in Fig. 2. It is a modification from Bouc-Wen model, which allows high adherence to the experimental data, especially for hysteresis behavior observed in the force $f^h_{mrd}(t)$ as a function of the relative speed between the ends of the damper - for this case $\dot{h}(t)$.

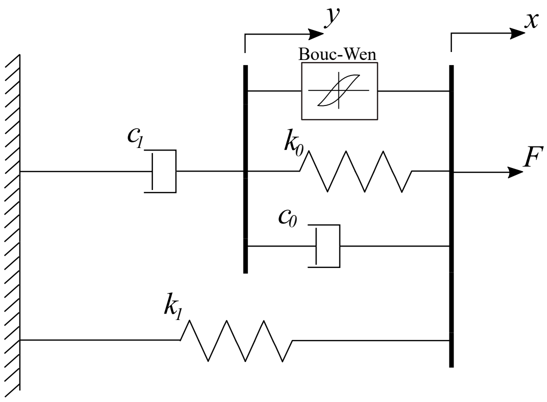

Figure 3. Magnetorheological damper model.
Source: adapted from Spencer Jr. *et al.* (1996).

$$f^h_{mrd}(t) = c_1^{mrd}\dot{y}(t) + k_1^{mrd}\left[h(t) - h_0\right] \tag{7}$$

where:

$$\dot{y}(t) = \frac{1}{\left(c_0^{mrd} + c_1^{mrd}\right)}\left[\alpha^{mrd}z(t) + c_0^{mrd}\dot{h}(t) + c_0^{mrd}\left(h(t) - y(t)\right)\right]$$

$$\dot{z} = -\gamma^{mrd}|\dot{h}(t) - \dot{y}(t)|z|z|^{n-1} - \beta^{mrd}\left[\dot{h}(t) - \dot{y}(t)\right]|z|^n + A^{mrd}\left[\dot{h}(t) - \dot{y}(t)\right]$$

The polynomials equations to change the Spencer parameters are defined as:

$$\begin{aligned} \alpha &= \alpha_a + \alpha_b u_{BW} \\ c_1 &= c_{1a} + c_{1b}u_{BW} \\ c_0 &= c_{0a} + c_{0b}u_{BW} \\ \dot{u}_{BW} &= -\eta(u_{BW} - E) \end{aligned} \tag{8}$$

where $z(t)$ is defined as an evolutionary variable, $y(t)$ is a displacement, α is the stiffness for the damping force associated with the variable z, k_0 and k_1 are the stiffness springs, c_0 and c_1 are the viscous damping coefficients, h_0 is the initial displacement of the spring with the stiffness k_0. β, γ, A and n are parameters for hysteresis control (Spencer Jr. *et al.*, 1996). E is the electrical voltage applied into the MRD. According with the Clipped-Optimal control method proposed by Dyke *et al.* (1996) presented in Fig. 2, the control law for the electrical voltage E applied to MRD is:

$$E = E_{max}\mathcal{H}(\{f_c(t) - f_{mrd}(t)\}f_{mrd}(t)) \tag{9}$$

where $\mathcal{H}(\cdot)$ is the Heaviside step function, $f_{mrd}(t)$ is the damping force associated to MRD, using the model proposed by Spencer Jr. *et al.* (1996), and $f_c(t)$ is the control force defined by the classic state feedback:

$$f_c(t) = -\mathbf{G}\mathbf{x}(t) \tag{10}$$

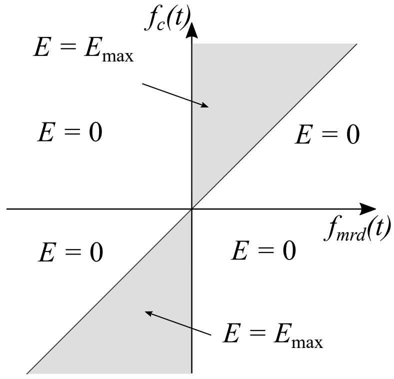

Figure 4. Electrical voltage calculation rule to determine magnetorheological force.
Source: adapted from Dyke *et al.* (1996).

where $\mathbf{G}$ is the control gain and $\mathbf{x}(t)$ is the state vector of the system. The command signal E is determined as follows: when the MRD providing the desired optimal force, i.e., $f_{mrd}(t) = f_c(t)$, the voltage should remain at the present level. If the magnitude of the force produced by the damper is smaller than the magnitude of the desired optimal force and the multiplication $f_{mrd}(t)f_c(t)$ is positive, the electrical voltage applied to the current driver is increased to the maximum level. Otherwise, the commanded voltage is set to zero (Dyke *et al.*, 1996). The control gain is obtained by solving the Lyapunov function for stability, where $\mathbf{X} = \mathbf{P}^{-1}$ and $\mathbf{B}_c = \mathbf{B}_m\{1 \quad 0 \quad 0\}^T$:

$$\mathbf{XA}^T - \mathbf{G}_x^T\mathbf{B}_c^T + \mathbf{AX} - \mathbf{B}_c\mathbf{G}_x < \mathbf{0} \tag{11}$$

where $\mathbf{G} = \mathbf{G}_x\mathbf{X}^{-1}$. This inequality is solved using the software CVX available in: `http://cvxr.com/cvx/`. A model representation is presented in Fig. 2, where through the gain $\mathbf{G}$ is possible determined the desirable control force, this is compared with the force applied to the damper, of this comparison, it is defined the electrical voltage value acting on the device.

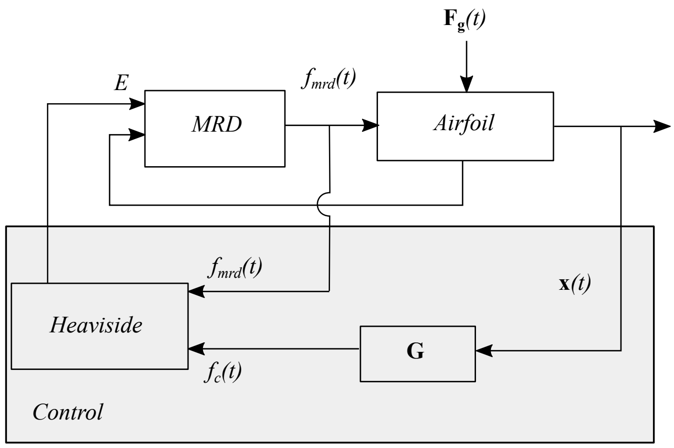

Figure 5. Feedback system with magnetorheological damper considering linear control force as reference.
Source: adapted from Dyke *et al.* (1996).

3. RESULTS AND DISCUSSIONS

The approach introduced in this article is evaluated considering the 3 DOF airfoil previously defined. The MR damper's parameters are shown in Tab. 2. Numerical simulations are carried out. Figure 6 shows the controlled and uncontrolled system responses for the thee degrees of freedom (dof), $h(t)$, $\theta(t)$ and $\beta(t)$. It is shown that MRD semi-ative strategy can reduce the maximum plunge displacement during the gust. Also, as shown in Fig. 7, the oscillating behavior verified for the uncontrolled condition, from the end of the gust, is suppressed when using the MRD device. However, Fig. 6 shows that the pitch and the control surface DOFs can achieve important level of oscillations also using the MRD fixed on the plunge degree of freedom.

Table 2. Parameters used to describe the magnetorheological damper force.

Parameters	**Values**	**Parameters**	**Values**
c_{0a}	210 [Ns/m]	α_a	1400 [N/m]
c_{0b}	35 [Ns/mV]	α_b	6950 [N/mV]
k_0	469 [Ns/m]	γ	363 [m^{-2}]
c_{1a}	2830 [Ns/m]	β	363 [m^{-2}]
c_{1b}	29.5 [Ns/mV]	A	301
k_1	50.0 [N/m]	n	2
h_0	0 [m]	η	190 [s^{-1}]

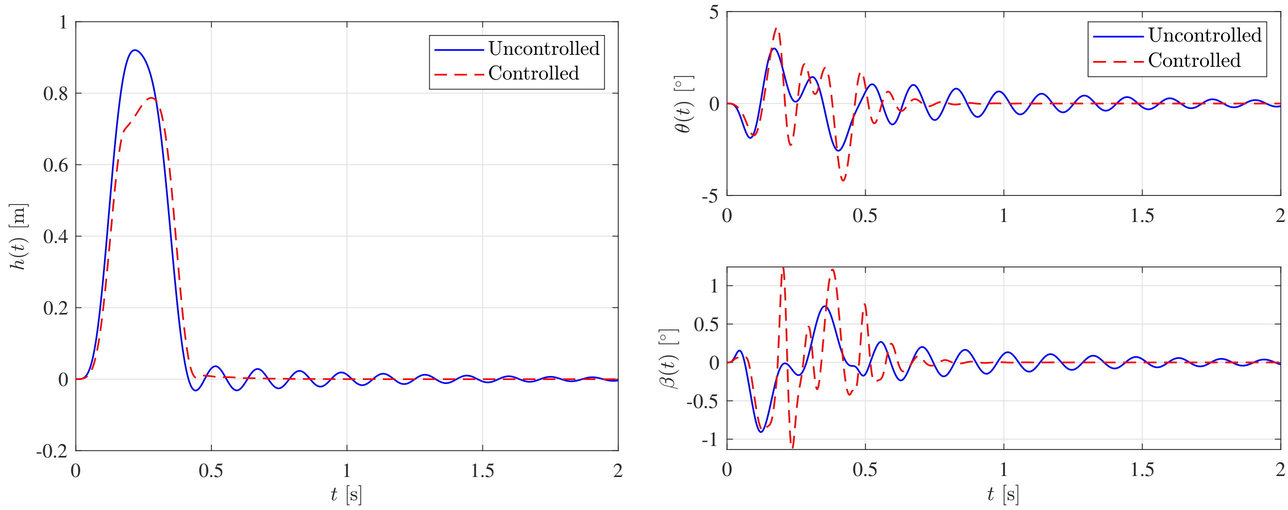

(a) Vertical displacement $h(t)$ in function of time (b) Rotation displacement $\theta(t)$ and $\beta(t)$ in function of time

Figure 6. Behavior of the system subject to gust efforts in time domain for passive and semi-active MRD conditions.

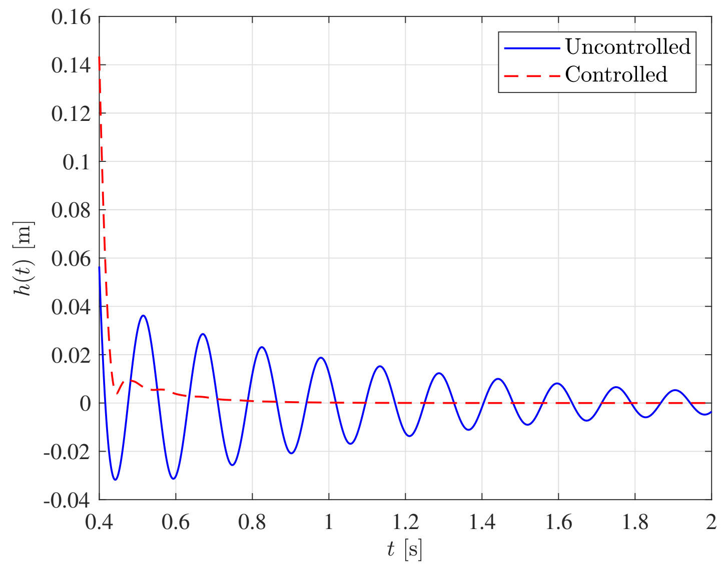

Figure 7. Rotation displacement $\theta(t)$ and $\beta(t)$ in function of time after gust.

Figure 8a shows the controller's force for the case previously presented. The MRD force achieves around 6 kN as maximum level. At the same figure, a classical feedback linear control (Eq. 10) is shown to compare the behavior of them. It is noted that, if the linear control is used to this case of gust, a higher level of maximum force is required. Also, both actuators operates during the similar time frame. However, the semi-active MRD technology using the clipped-optimal approach requires an abrupt change of the electrical voltage applied on it over time, as shown in Fig. 8b, and this characteristic can degrade the operating lifetime of this device.

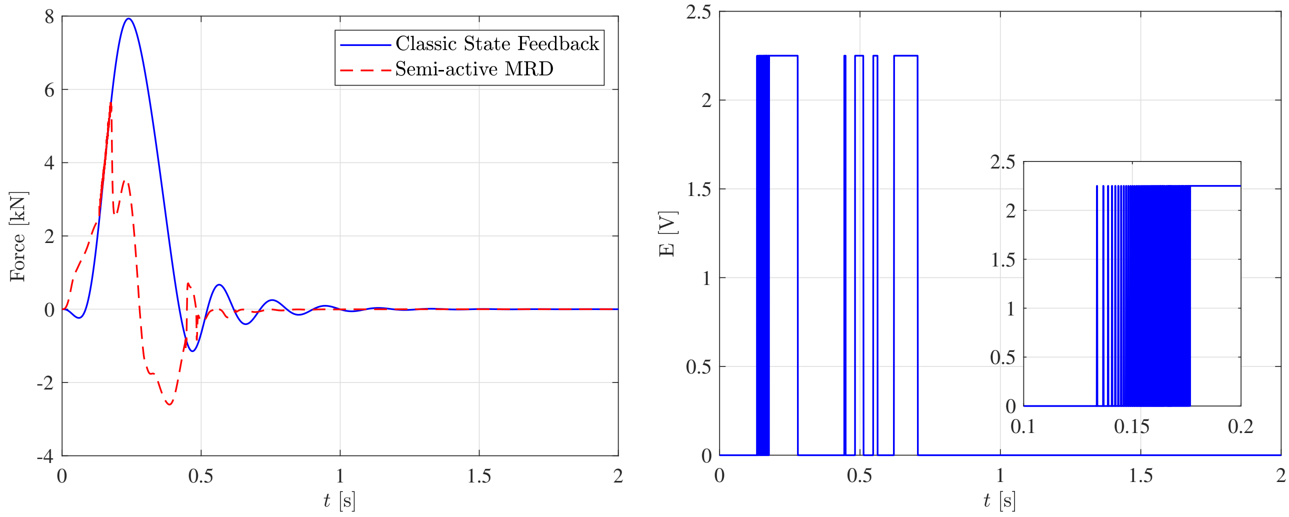

(a) Damping force for controlled, passive and semi-active MRD conditions

(b) Input voltage for semi-active MRD condition

Figure 8. Damping force and voltage in function of time

Figures 9a and 9b show the maximum displacement of plunge, $\max(h) = h_{max}$ for different values of gust gradient (H) and air speeds (V), respectively. Considering $V = 80$ m/s, Fig. 9a demonstrates that MRD device is good choice to reduce the maximum plunge displacement during the gust action, mainly if $H < 25$ m - for this systems parameters. Similar performance is verified in Fig. 9b considering $H = 37$ meters.

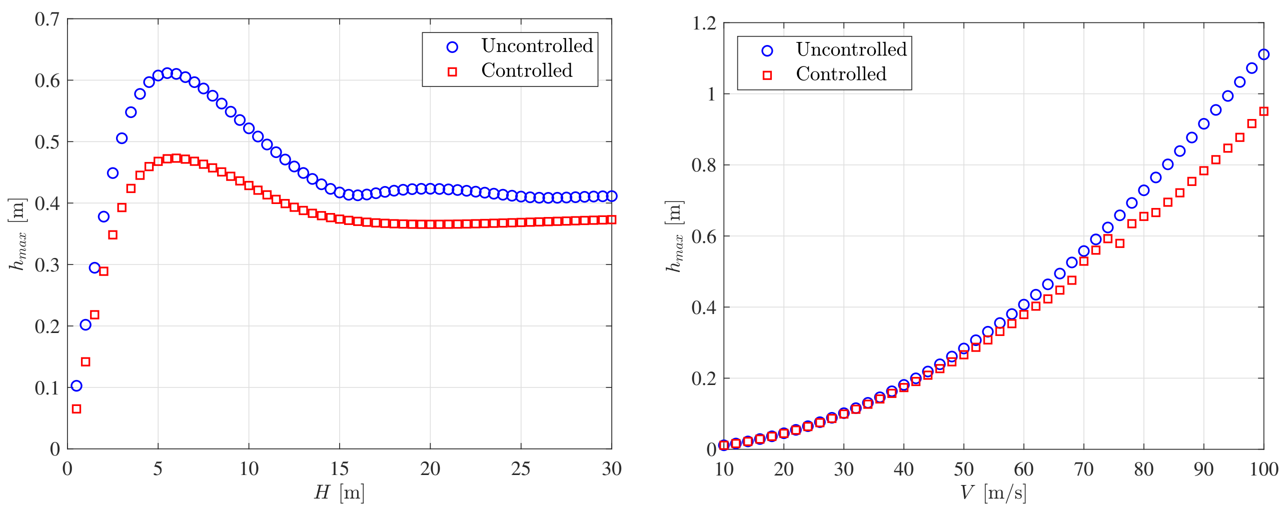

(a)

(b)

Figure 9. Maximum displacement of plunge in term of: (a) gust gradient; (b) airspeed.

4. FINAL REMARKS

This work shows the hybrid and non conventional approach to suppress gust combining the use of a magnetorheological damper and linear matrix inequalities. It is considered a 3 DOF airfoil described in the time domain using the state space representation and considering unsteady aerodynamic written in time domain using Roger-Abel rational function approximation-based method. It is introduced the LMI-based technique to get the control gain and it is used the Clipped-Optimal method to set the MRD force over time. The results show that MRD devices are a good choice to suppress 1-cosine gust. However, it can require abrupt change of electrical voltage applied on it over time, which can degrade the lifetime of this type of device.

5. ACKNOWLEDGEMENTS

The authors would like to express their appreciation to CAPES and FAPESP (2016/20617-0 process) for supporting this research.

6. REFERENCES

Abel, I., 1979. "An analytical technique for predicting the characteristics of a flexible wing equipped with an active flutter-suppression system and comparison with wind-tunnel data". Technical report, National Aeronautics and Space Administration - NASA.

Bisplinghoff, H.A., Raymond, L. and Halfman, R.L., 1996. *Aeroelasticity*. Dover Publications, INC.

Chen, P.C., 2000. "Damping perturbation method for flutter solution: The g-method". *AIAA Journal*, Vol. 38, pp. 1519–1524.

Dyke, S.J., Spencer, B.F., Sain, M.K. and Carlson, J.D., 1996. "Modeling and control of magnetorheological dampers for seismic response reduction". *Smart Materials and Structures*, Vol. 5, pp. 565–575.

Dyke, S.J., Spencer Jr., B.F., Sain, M..K. and Carlson, J.D., 1998. "An experimental study of mr dampers for seismic protection". *Smart Materials and Structures: Special Issue on Large Civil Structures*, Vol. 7, No. 5, pp. 693–703.

Guo, S., Monteros, J.E. and Liu, Y., 2015. "Gust alleviation of a large aircraft with a passive twist wingtip". *Aerospace*, Vol. 2, No. 2, pp. 135–154.

Jansen, L.M. and Dyke, S.J., 2000. "Semi-active control strategies for mr dampers: A comparative study". *ASCE Journal of Engineering Mechanics*, Vol. 126, No. 8, pp. 795–803.

Karpel, M., 1981. "Design for active and passive flutter suppression and gust alleviation". TR 3482, National Aeronautics and Space Administration - NASA.

Lord, 2009. "Lord technical data: Rd-8040-1 and rd-8041-1 dampers".

Regan, C.D. and Jutte, C.V., 2012. "Survey of applications of active control technology for gust alleviation and new challenges for lighter-weight aircraft". TM 2012-216008, National Aeronautics and Space Administration (NASA).

Roger, K., 1977. "Airplane math modelling methods for active control design". *AGARD Conference Proceeding*, Vol. 9, pp. 4.1–4.11.

Spencer Jr., B.F., Dyke, S.J., Sain, M..K. and Carlson, J.D., 1996. "Phenomenological model of a magnetorheological damper". *ASCE Journal of Engineering Mechanics*, Vol. 123, No. 1-23, pp. 230–238.

Suleman, A. and Costa, A.P., 2004. "Adaptive control of an aeroelastic flight vehicle using piezoelectric actuators". *Computers & Structures*, Vol. 82, No. 17-19, pp. 1303–1314.

Theodorsen, T., 1935. "General theory of aerodynamic instability and the mechanism of flutter". *NACA Rept. 496*, Vol. 13, pp. 374–387.

Wright, J. and Cooper, J., 2007. *Introduction to Aircraft Aeroelasticity and Loads*. AIAA education series. John Wiley & Sons. ISBN 9781563477225.

7. RESPONSIBILITY NOTICE

The authors are the only responsible for the printed material included in this paper.

A STATE SPACE MATRICES

The aeroelastic dynamic matrix of the system $\mathbf{A}$ with the augmented states is given by:

$$\mathbf{A} = \begin{bmatrix} -\mathbf{M}_a\mathbf{B}_a & -\mathbf{M}_a\mathbf{K}_a & q\mathbf{Q}_3 & \cdots & q\mathbf{Q}_{2+n_{lag}} \\ \mathbf{I} & \mathbf{0} & \mathbf{0} & \cdots & \mathbf{0} \\ \mathbf{I} & \mathbf{0} & -\frac{V}{b}\gamma_1\mathbf{I} & \cdots & \mathbf{0} \\ \vdots & \vdots & \mathbf{0} & \ddots & \cdots \\ \mathbf{I} & \mathbf{0} & \vdots & \cdots & -\frac{V}{b}\gamma_{n_{lag}}\mathbf{I} \end{bmatrix} \tag{12}$$

where,

$$\mathbf{M}_a = \mathbf{M} - q\frac{b^2}{V^2}\mathbf{Q}_2 \tag{13}$$

$$\mathbf{B}_a = \mathbf{B} - q\frac{b}{V}\mathbf{Q}_1 \tag{14}$$

$$\mathbf{K}_a = \mathbf{K} - q\mathbf{Q}_0 \tag{15}$$

$\mathbf{I}$ is the identity matrix and $\mathbf{0}$ is a zero matrix.

Through the representation in the space of states, $\mathbf{B}_m$ and $\mathbf{B}_g$ matrices present the following form:

$$\mathbf{B}_m = \begin{bmatrix} -\mathbf{M}^{-1} \\ \mathbf{0} \end{bmatrix} \tag{16}$$

$$\mathbf{B}_g = \begin{bmatrix} \mathbf{M}^{-1} \\ \mathbf{0} \end{bmatrix} \tag{17}$$